Bioorganic & Medicinal Chemistry Letters 30 (2020) 126915

Contents lists available at ScienceDirect

Bioorganic & Medicinal Chemistry Letters

journal homepage: www.elsevier.com/locate/bmcl

# Evaluation of $^{64}$Cu radiolabeled anti-hPD-L1 Nb6 for positron emission tomography imaging in lung cancer tumor mice model

Jinquan Jiang[a,d], Meixin Zhang[a,b,d], Guanghui Li[c], Teli Liu[a], Yakun Wan[c], Zhaofei Liu[b], Hua Zhu[a,*], Zhi Yang[a,*]

[a] Key Laboratory of Carcinogenesis and Translational Research (Ministry of Education/Beijing), Department of Nuclear Medicine, Peking University Cancer Hospital & Institute, Beijing 100142, PR China
[b] Department of Radiation Medicine, School of Basic Medical Science, Peking University, Beijing 100191, PR China
[c] Shanghai Novamab Biopharmaceuticals Co., Ltd., Shanghai 201203, PR China

ARTICLE INFO

*Keywords:*
Heavy chain-only antibody (HCAb)
$^{64}$Cu-NOTA-Nb6
PD-L1
Lung cancer
PET/CT imaging

ABSTRACT

Recently, we selected a novel anti-hPD-L1-specific HCAb named Nb6 with high affinity ($EC_{50}$ = 0.65 ng/mL) for potential hPD-L1 targeted non-invasive PET imaging. In this research, Nb6 was conjugated with the bifunctional chelator NCS-Bz-NOTA ((2-[(4-Isothiocyanophenyl) methyl]-1,4,7-triazacy-clononane-1,4,7-triacetic acid)) and further labeled with radio-nuclide $^{64}$Cu. $^{64}$Cu-NOTA-Nb6 was prepared with over 95% labeling yield, over 99% radiochemical purity and 14–16 GBq/μmol specific activity after PD-10 column purification. It shows good stability in 0.01 M PBS and 5% HSA solutions. $^{64}$Cu-NOTA-Nb6 has a high binding affinity to 3.60 nM which was tested by human lung adenocarcinoma A549 cell lines. Tumor lesion can be clearly observed from 20 h to 38 h by Micro-PET equipment after $^{64}$Cu-NOTA-Nb6 administration. The study revealed that $^{64}$Cu-NOTA-Nb6 has good lesion detection ability, high ratios between tumor and non-tumor signal and can specifically target A549 xenografted tumor model. Taken together of good stability, high binding affinity, and tumor detection ability, $^{64}$Cu labeled Nb6 is a promising radio-tracer in diagnosing of hPD-L1 overexpression tumor, supposed to monitor PD-L1overexpression tumor progression and guide targeted therapy with PET molecular imaging.

Among cancers, lung cancer is the leading cause of death worldwide.[1,2] Non-small cell lung cancer (NSCLC) accounts for the vast majority of lung cancer. The traditional treatment of NSCLC is surgery, radiotherapy, and chemotherapy, to which the response of tumors is poor and may have great side effects. Therefore, the diagnosis, the evaluation of treatment and the prognosis of lung cancer are particularly important. With the rise of immunotherapy, many inhibitors of immune checkpoint have been developed, among which anti-PD-1/PD-L1 antibodies provide a new idea for the treatment of NSCLC. However, there are some problems in immunotherapy-based on anti-PD-1/PD-L1 antibodies. No response was shown in many NSCLC patients and even serious immune-related adverse reactions were observed.[3,4]

Fortunately, PD-L1 expression by Immunohistochemistry (IHC), the main pathological examination and clinical diagnosis for cancer patients, correlates with response and survival following the PD-L1 monoclonal antibody (mAb) immunotherapy.[4] Therefore, accurate examination of PD-L1 expression in tumors is the key to NSCLC immunological checkpoint inhibitors treatments. Due to the heterogeneity[5,6] and dynamic expression of tumor-associated antigens or tumor-specific antigens, IHC has limitations in PD-L1 expression. But semi-quantitative molecular imaging technology Positron Emission Tomography Computed Tomography (PET/CT),[7,8] with its high sensitivity, specificity, whole-body imaging and safety,[9] can provide near-real-time information about receptors' expression levels and take patients' individual response into account, allowing doctors to predict which patients may benefit from immunotherapy, therefore avoiding ineffective treatment and adverse effect.

With the advent of PET/CT, the study of PET/CT molecular probes is flourishing in clinical diagnosis and cancer treatments. Even studies of Nbs whose relative molecular mass are only about 12–15 kDa have been carried out.

Nbs was discovered in 1993 by Hamers Casterman.[10] Hamers Casterman's team found a large number of heavy chain-only antibodies (HCAbs) in the serum of camels. HCAbs lacked light chains and contained only heavy-chain. The variable region of heavy chain equipped with antigen-binding activity in HCAbs was extracted and used as a new

* Corresponding authors.
*E-mail addresses:* jiangjinquan1989@163.com (H. Zhu), pekyz@163.com (Z. Yang).
[d] Equal contribution.

https://doi.org/10.1016/j.bmcl.2019.126915
Received 29 October 2019; Received in revised form 3 December 2019; Accepted 16 December 2019
Available online 24 December 2019
0960-894X/ 

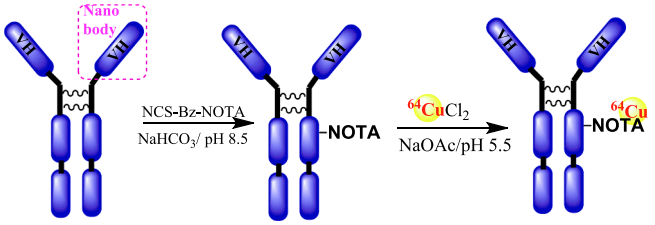


**Fig. 1.** The labeling procedure of $^{64}$Cu-NOTA-Nb6.

antibody, also known as a single-domain antibody (sdAb) or variable domain of the heavy-chain of heavy-chain antibody (VHH).[11] In addition to weak immunogenicity, nanobodies have high affinity and specificity, good solubility, improved stability, well-performed acid-resistance.[12] And compared with monoclonal antibodies, nanobodies have a higher penetration rate in tissues and can be quickly cleared through the kidney.[13] Now, nanobodies are widely used in molecular imaging. For example, Broos K[14] and his team have undertaken non-invasive SPECT/CT imaging murine tumor models with positive PD-L1 expression by using 99mTc-labeled PD-L1-specific Nbs.

The Nb6 (relative molecular mass is 77837.357 Da) used in this research is two anti-hPD-L1 VHHs linking with Fc.[12] Most recently, we reported the I-124 radio-labeled PD-L1 Nb6 is useful for non-invasive PET imaging in the osteosarcoma tumor model.[15] Here, we produced $^{64}$Cu-NOTA-Nb6 and applied it to PET molecular imaging. The synthesis and labeling process is shown in Fig. 1.

The $1 \times 10^{-5}$ mol Nb6 was reacted with $5 \times 10^{-5}$ mol bifunctional chelator NCS-Bz-NOTA whose relative molecular mass is 450.5 Da overnight at pH 8.0–8.5 0.1 M $NaHCO_3$ solutions. The product was purified through a disposable PD-10 desalting column. The concentrations of collected protein were measured by a NanoDrop 2000 UV–Visible Spectrophotometer; the relative molecular mass of Nb6 and modified Nb6 were measured by MALDI-TOF-MS. The results showed each Nb6 antibody was conjugated with 1.13 NCS-Bz-NOTA on average (Fig. 2).

We produced the radionuclide $^{64}$Cu with the total radioactivity greater than 150 mCi and specific activity 5.6 GBq/μ moL.4.60 nmol NOTA-Nb6 was radiolabeled with 74 GBq $^{64}$CuCl2 at pH 5.5 0.1 M NaAc solutions under room temperature for 30 min. 5 μL product was taken as a tested sample mixed with saturated EDTA and developed through 0.9% NaCl developing solvent. And then tested by Radio-TLC, which suggested over 95% labeling yield and over 99% radiochemical purity after purified through disposable PD-10 desalting column (Fig. 3). The specific activity was 14–16 GBq/μmol by calculation.

The stability of $^{64}$Cu-NOTA-Nb6 was tested through Radio-TLC. After placed in Phosphate Buffered Saline (PBS) and human serum albumin (HSA) separately for 12 h, 100% $^{64}$Cu-NOTA- Nb6 retained its original structure. The radio chemical purity of $^{64}$Cu-NOTA-Nb6 was up to 97.97% after placed in PBS for 18 h and 88.97% after 36 h at 37 °C. And after placed in HSA for 18 h and 36 h, the radiochemical purity of $^{64}$Cu-NOTA-Nb6 was up to 97.23% and 95.43% respectively (Fig. 4), indicating that $^{64}$Cu-NOTA-Nb6 performed well in vitro stability in both PBS and HSA and can be placed in vitro for a long period of time before application.

Saturation binding studies were performed with $^{64}$Cu-NOTA-Nb6 in A549 lung tumor cell lines. Eight test A549 lung tumor cell solutions (n = 4) were incubated in $^{64}$Cu-NOTA-Nb6 from the 1.4 nM to 28.1 nM. The incubating medium in two 24-well plates was removed before 2 h of experiment. And added a new medium containing no fetal bovine serum (FBS), replacing 24-well plates in a 37 °C incubator. After 2 h, A549 lung tumor cells were exposed to increasing concentrations of $^{64}$Cu-NOTA-Nb6 (1.4 nM to 28 nM) and in a total volume of 320 μL 1% PBS (pH 7.4) for 2 h at 37 °C, and then washed three times with ice-cold 1% PBS. Digested and lysis cell with 350 μL 1 M NaOH for 3 min and tested radioactivity of each solution. Data were analyzed through Graph Pad Prism Software to determine the $K_d$ and Bmax values. The Bmax values were 5165 and the $K_d$ was 3.60 nM, according to a one-site binding model (Fig. 5). The result indicates that $^{64}$Cu-NOTA-Nb6 can specifically bind A549 lung tumor cells with good affinity.

We chose A549 xenografted tumor model as our experimental mice. After injecting A549 tumor-bearing mice with 14.8 MBq $^{64}$Cu-NOTA-Nb6, we collected Micro-PET images at 2 h, 6 h, 20 h, and 38 h and 50 h post-injection, which are shown in Fig. 6(a–c). The images were reconstructed and analyzed by Sedecal 3D OSEM system. The standard uptake value (SUV) means of tumor, lung, heart, liver, muscle, thyroid, the brain was analyzed by Image. According to the imaging results, it was speculated that some $^{64}$Cu-NOTA-Nb6 was still circulating in the blood within 6 h after injection, and some were metabolized by the liver, but $^{64}$Cu-NOTA-Nb6 did not fully combine with the tumor. $^{64}$Cu-NOTA-Nb6 was further metabolized through the liver over time. The accumulation of $^{64}$Cu-NOTA-Nb6 in the liver was getting growingly higher, and the accumulation in the tumor was gradually increasing. The SUVmean ratios of T/NT gradually increased with time. The SUVmean ratios of tumor/heart increased from 0.218 to 2.062, and that of tumor/liver raised from 0.149 to 1.604, as shown in Fig. 6(d). The images and the SUVs showed that before 20 h, $^{64}$Cu-NOTA-Nb6 has not fully combined with tumors. After 38 h, due to the decay of $^{64}$Cu (t1/2 = 12.7 h), the resolution ratio of Micro-PET images is low, which is not appropriate to observe, Therefore, the observation of tumors

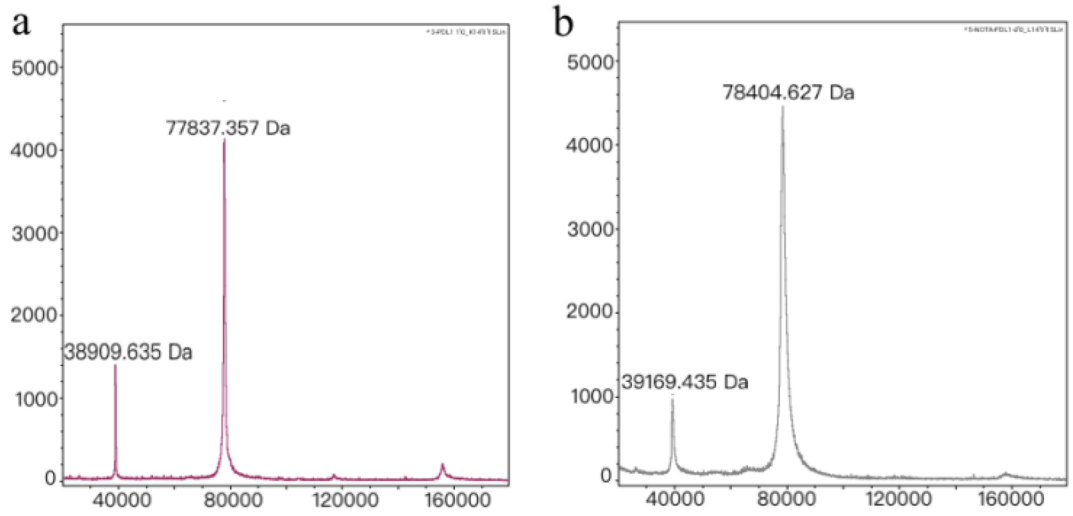


**Fig. 2.** MALDI-TOF Mass Spectrometric Charts of Nb6 (a) and NCS-Bz-NOTA-Nb6 (b).

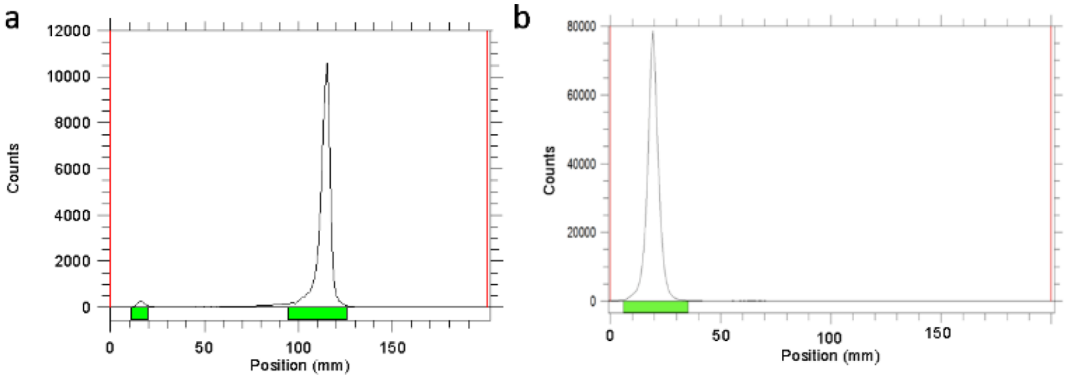


**Fig. 3.** Radio-TLC imagine of $^{64}CuCl_2$ (a); Radio-TLC chromatograms of $^{64}$Cu-NOTA-Nb6 (b).

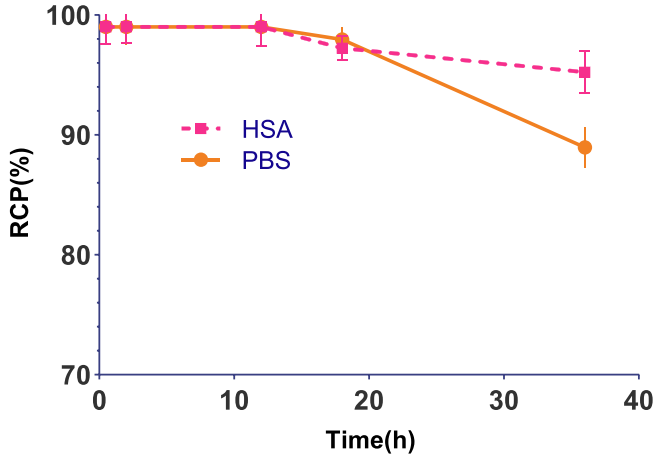


**Fig. 4.** Radiochemical purity (RCP) of $^{64}$Cu-NOTA-Nb6 in PBS and HSA system respectively tested by Radio-TLC.

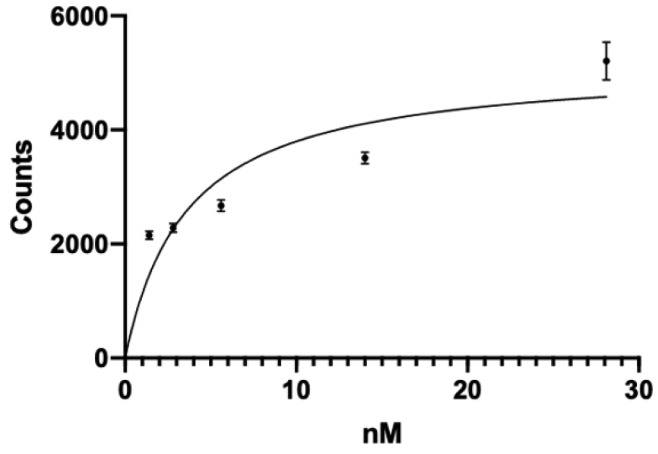


**Fig. 5.** Binding affinity measurement of $^{64}$Cu-NOTA-Nb6 to A549 lung tumor cells. A549 lung tumor cells were exposed to increasing concentrations of $^{64}$Cu-NOTA-Nb6 for 2 h at 37 °C.

between 20 h to 38 h after the injection is best.

Our previously report[15] confirmed that $^{124}$I-anti-hPD-L1 Nb6 may provide a novel strategy to screen osteosarcoma patients. However, $^{124}$I is not easily available and has a long half-life of 4.176 D. Compared with $^{124}$I, $^{64}$Cu is more readily available and has a shorter half-life 12.7 h, which better matches the metabolic time of NB6 and is convenient for clinical use, and the radiation dose is low. In our experiments, results indicate with the circulations of this $^{64}$Cu-NOTA-Nb6 probe, tumor to normal organ ratios increased from 2 to 50 h.

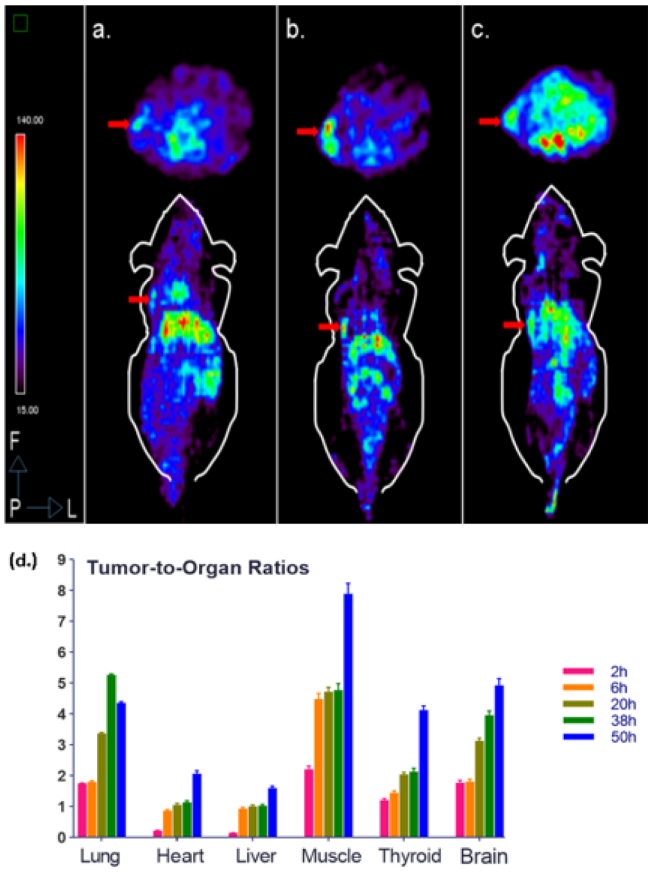


**Fig. 6.** Micro-PET imaging of the $^{64}$Cu-NOTA-Nb6 in mice bearing A549 tumors. The Micro-PET images were collected at 2 h, 6 h (a), 20 h (b), 38 h (c) and 50 h. The tumor was pointed out with red arrows. T/NT(n = 3) SUVmean ratios at each time point after injection of $^{64}$Cu-NOTA-Nb6 (d). (For interpretation of the references to colour in this figure legend, the reader is referred to the web version of this article.)

Combined with 4.2 nM $K_d$ value in cell binding experiments. $^{64}$Cu-NOTA-Nb6 exhibits tumor-targeting ability in lung cancer A549 xenograft mice models.

In summary, this research successfully demonstrates that $^{64}$Cu can label NOTA-Nb6 with high labeling yield and specific activity. $^{64}$Cu-NOTA-Nb6 is equipped with great stability in vitro, satisfactory affinity to A549 lung tumor cells. The Micro-PET images suggested that $^{64}$Cu-NOTA-Nb6 concentrated highly in A549 lung tumor, and 20 h to 38 h post-injection is best for observation. All results approved that $^{64}$Cu-NOTA-Nb6 is a promising probe in NSCLC diagnosis, lesion detection and guidance of targeted therapy with PET molecular imaging. It is

possible to stratify cancers and predict the prognosis of NSCLC in the clinic with $^{64}$Cu-NOTA-Nb6 so as to assist doctors in determining treatment strategies and to reduce ineffective treatment as well as avoid potential side effects. Nb6 can also be used in combined clinical treatments of tumors, which is expected to achieve clinical transformation in a short time.

## Declaration of Competing Interest

The authors declare that they have no known competing financial interests or personal relationships that could have appeared to influence the work reported in this paper.

## Acknowledgments

This work was supported by a grant from the National Natural Science Foundation of China (No. 81401467, 81731592). Beijing Nova Program (Z171100001117020), the Beijing Excellent Talents Funding (2017000021223ZK33), Open Project funded by Key Laboratory of Carcinogenesis and Translational Research, Ministry of Education/Beijing (2017 open project-1 and 2019 open project-06).

## References

1. McIntyre AGA. Lung cancer-a global perspective. *Surg Oncol.* 2017;115:550–554.
2. Torre LA SR, Jemal A. Lung cancer statistics. *Adv Exp Med Biol.* 2016;893:1–19.
3. Acurcio RC, Scomparin A, Conniot J, et al. Structure-function analysis of immune checkpoint receptors to guide emerging anticancer immunotherapy. *J Med Chem.* 2018;61:10957–10975. https://doi.org/10.1021/acs.jmedchem.8b00541.
4. Niemeijer AN, Leung D, Huisman MC, et al. Whole-body PD-1 and PD-l1 positron emission tomography in patients with non-small-cell lung cancer. *Nat Commun.* 2018;9:4664. https://doi.org/10.1038/s41467-018-07131-y.
5. Büttner R, Gosney JR, Skov BG, et al. Programmed death-ligand 1 immunohistochemistry testing: a review of analytical assays and clinical implementation in non–small-cell lung cancer. *J Clin Oncol.* 2017;35:3867–3876. https://doi.org/10.1200/jco.2017.74.7642.
6. Ilie M, Long-Mira E, Bence C, et al. Comparative study of the PD-l1 status between surgically resected specimens and matched biopsies of nsclc patients reveal major discordances: a potential issue for anti-PD-l1 therapeutic strategies. *Ann Oncol.* 2016;27:147–153. https://doi.org/10.1093/annonc/mdv489.
7. Bensch F, van der Veen EL, Lub-de Hooge MN, et al. (89)zr-atezolizumab imaging as a non-invasive approach to assess clinical response to PD-l1 blockade in cancer. *Nat Med.* 2018;24:1852–1858. https://doi.org/10.1038/s41591-018-0255-8.
8. Xing Y, Chand G, Liu C, et al. Early phase I study of a 99mtc-labeled anti-programmed death ligand-1 (PD-l1) single-domain antibody in spect/ct assessment of PD-l1 expression in non–small cell lung cancer. *J Nucl Med.* 2019;60:1213–1220. https://doi.org/10.2967/jnumed.118.224170.
9. Ehman EC, Johnson GB, Villanueva-Meyer JE, et al. Pet/MRI: Where might it replace pet/ct? *J Magn Reson Imaging.* 2017;46:1247–1262. https://doi.org/10.1002/jmri.25711.
10. Hamers-Casterman C, Atarhouch T, Muyldermans S, et al. Naturally occurring antibodies devoid of light chains. *Nature.* 1993;363:446–448. https://doi.org/10.1038/363446a0.
11. Arbabi-Ghahroudi M. Camelid single-domain antibodies: Historical perspective and future outlook. Front Immunol. 2017;8. doi: 10.3389/fimmu.2017.01589.
12. Li G, Zhu M, Ma L, et al. Generation of small single domain nanobody binders for sensitive detection of testosterone by electrochemical impedance spectroscopy. *ACS Appl Mater Interfaces.* 2016;8:13830–13839. https://doi.org/10.1021/acsami.6b04658.
13. Klein A, Kovacs M, Muskotal A, et al. Nanobody-displaying flagellar nanotubes. *Sci Rep.* 2018;8:3584. https://doi.org/10.1038/s41598-018-22085-3.
14. Broos K, Keyaerts M, Lecocq Q, et al. Non-invasive assessment of murine pd-l1 levels in syngeneic tumor models by nuclear imaging with nanobody tracers. Oncotarget 2017;8:41932–41946. doi: 10.18632/oncotarget.16708.
15. Huang HF, Zhu H, Li GH, et al. Construction of anti-hpd-l1 hcab nb6 and in situ (124) i labeling for noninvasive detection of pd-l1 expression in human bone sarcoma. *Bioconjug Chem.* 2019;30:2614–2623. https://doi.org/10.1021/acs.bioconjchem.9b00539.